

## Minimizing the filtration loss of water-based drilling fluid with sustainable basil seed powder

Hanyi Zhong<sup>a, b, \*</sup>, Xin Gao<sup>a, b</sup>, Xianbin Zhang<sup>c</sup>, Anliang Chen<sup>c</sup>, Zhengsong Qiu<sup>a, b</sup>, Xiangzheng Kong<sup>a, b</sup>, Weian Huang<sup>a, b</sup>

<sup>a</sup> Key Laboratory of Unconventional Oil & Gas Development (China University of Petroleum (East China), Ministry of Education, Qingdao, 266580, China

<sup>b</sup> School of Petroleum Engineering, China University of Petroleum (East China), Qingdao, Shandong, 266580, China

<sup>c</sup> Drilling Fluid Technology Services of CNPC Bohai Drilling Engineering Company Limited, Dagang, Tianjin, 300280, China

### ARTICLE INFO

#### Article history:

Received 21 August 2020

Received in revised form

31 October 2020

Accepted 3 February 2021

#### Keywords:

Bentonite suspension

Basil seed

Filtration

Interaction

Water-based drilling fluid

### ABSTRACT

Filtration control is important to ensure safe and high efficient drilling. The aim of the current research is to explore the feasibility of using basil seed powders (BSPs) to reduce filtration loss in water-based drilling fluid. The effect of BSP concentration, thermal aging temperature, inorganic salts (NaCl and CaCl<sub>2</sub>) on the filtration properties of bentonite/basil suspensions was investigated. The filtration control mechanism of BSP was probed via water absorbency test, zeta potential measurement, particle size distribution measurement, and filter cake morphologies observation by scanning electron microscope. The incorporation of BSPs into the bentonite suspension generated acceptable rheology below 1.0 w/v%. The BSPs exhibited effective filtration control after thermal aging at 120 °C, but less efficiency at 150 °C. After thermal aging at 120 °C, the bentonite suspension containing 1.0 w/v% BSPs could resist NaCl and CaCl<sub>2</sub> pollution of 5.0 w/v% and 0.3 w/v% respectively. Besides general filtration control behaviors, the exceptional water retaining capability formed by numerous nanoscale 3D networks in the basil seed gum and considerable insoluble small particles in BSPs might further contribute to the filtration control. The excellent filtration properties bring basil seed a suitable and green candidate for the establishment of high-performance drilling fluids.

© 2021 Southwest Petroleum University. Production and hosting by Elsevier B.V. on behalf of KeAi Communications Co., Ltd. This is an open access article under the CC BY-NC-ND license (<http://creativecommons.org/licenses/by-nc-nd/4.0/>).

### 1. Introduction

Drilling fluids are important in oil and gas drilling operation including preserving acceptable rheological properties, stabilizing well-bore, carrying drill cuttings from down-hole to surface and preventing reservoir damage [1–3]. Generally water-based, oil-based and synthetic-based drilling fluid are three categories of drilling fluids mostly used. Although having the intrinsic merits of elevated temperature stability, exceptional lubricity and

outstanding shale hydration inhibitive capacity, the high cost and potential adverse effect on environment limit the wide use of oil-based drilling fluid. Consequently water-based drilling fluids are used predominantly around the world because of their low cost, environmental friendly, and facile preparation compared to other drilling fluids [4].

Water-based drilling fluid is mainly composed of water, bentonite, polymers, salts and other components to maintain the required properties in drilling. Among the various properties, effective filtration control is important since a thin filter cake will form on the wellbore surface, which can avoid the filtrate leaking into the formation, maintain the wellbore stability and minimize the reservoir damage [5].

During the past decades, many types of filtration loss reducers have been utilized to reduce the filtration loss of water-based drilling fluid into formations. Various particles with different sizes such as calcium carbonate, graphite, polymer microspheres are capable of plugging the micro-pores and decrease the drilling

\* Corresponding author. School of Petroleum Engineering, China University of Petroleum, Qingdao, 266580, China.

E-mail address: [zhonghanyi@126.com](mailto:zhonghanyi@126.com) (H. Zhong).

Peer review under responsibility of Southwest Petroleum University.



Production and Hosting by Elsevier on behalf of KeAi

<https://doi.org/10.1016/j.petlm.2021.02.001>

2405-6561/© 2021 Southwest Petroleum University. Production and hosting by Elsevier B.V. on behalf of KeAi Communications Co., Ltd. This is an open access article under the CC BY-NC-ND license (<http://creativecommons.org/licenses/by-nc-nd/4.0/>).

Please cite this article as: H. Zhong, X. Gao, X. Zhang *et al.*, Minimizing the filtration loss of water-based drilling fluid with sustainable basil seed powder, *Petroleum*, <https://doi.org/10.1016/j.petlm.2021.02.001>

fluid invasion. Asphaltic additives can also seal the micro pores by softening and deformation. Polymers, mainly including two types of synthetic and natural, are the most widely used because they can be employed to optimize the rheological and filtration properties simultaneously by interaction with clay particles and improvement of the quality of filter cake [6]. Due to the characteristic of general biodegradability, environmental friendliness, renewability, abundance in nature and availability at a low cost, the biopolymers are typically applied to improve the rheological and filtration properties of water-based drilling fluids. Some examples include starch, cellulose, lignite, guar, xanthan, diutan, carrageenan, scleroglucan, sesbania gum, psyllium husk, and welan as well as their chemically modified analogues [4,7–10]. With the aim of developing environmental-friendly water-based drilling fluids with high performance, there is still a progressive requirement for natural biopolymer additives which are able to effectively control the filtration loss into the subterranean formation.

*Ocimum basilicum* L., also named as basil, is a universal herb plant grown in many parts of the world particularly in the tropical regions [11]. The basil seed presents black and oval. The length, width and thickness are  $3.22 \pm 0.33$  mm,  $1.84 \pm 0.24$  mm and  $1.37 \pm 0.15$  mm, respectively. The primary composition of the basil seed includes carbohydrate (47–50%), lipid (22–25%) and protein (18–20%) [12]. Due to the existence of a polysaccharide layer in the outer pericarp of basil seed, the basil seed would swell into a gelatinous mass after soaking in water. The acid-stable portion of glucomannan (43%) with glucose and mannose at ratio of 10:2 and the acid-dissolved portion of (1 → 4)-linked xylan (24.29%) are the two major polysaccharides fractions extracted from the basil seed. Meanwhile, small quantities of glucan (2.31%) and highly branched arabinogalactan are also detected in basil seed [13,14]. Since the amount of hydrocolloid in basil seed is high, it is appealing to compare the basil seed gum with commercial gums like xanthan gum [15]. At present, the researches related to basil seed gum are primarily focused on medicine, cuisine and chemical properties [14]. There are few works reporting the use of basil seeds to improve the filtration loss control in petroleum drilling engineering.

The interaction between bentonite platelets and polymers are critically important since it exhibits fundamental influence on the properties of water-based drilling fluid. Therefore, in the present research, the influence of different factors such as basil seed powder (BSP) concentration, thermal aging temperature, and inorganic salts (NaCl and CaCl<sub>2</sub>) on the filtration properties of bentonite suspension was probed, followed by the characterization of the interaction between BSP and bentonite particles with zeta potential test, particle size distribution measurement and filter cake morphology observation by scanning electron microscope (SEM). Finally, the underlying mechanism of using BSPs to control filtration loss in water-based drilling fluid was proposed.

## 2. Materials and methods

### 2.1. Materials

Basil seeds were bought from Bozhou rose fragrance Biotechnology Co., Ltd, China. Sodium bentonite (Na-bent) complying with the API standard was provided by Weifang Huawei bentonite Group Co., Ltd, China. Sodium chloride, calcium chloride, sodium carbonate and anhydrous ethanol in analytical grade were purchased from Sinopharm Chemical Reagent Co., Ltd, China. All the experimental materials were used as received.

### 2.2. Pretreatment of basil seed

Basil seeds were crushed by a grinder at a stirring rate of 27000 rpm for 1 min and an intermediate pause of 1 min. After grinding of 10 min, the crushed powder was washed with anhydrous ethanol for several times until the filtrate became colorless. The filtered powder was dried at 80 °C for 2 h. The dried powder was crushed and washed with anhydrous ethanol again following the above procedure. Finally all the BSPs sieved through 40 mesh was obtained.

### 2.3. Water absorption capacity

BSPs (1.0 g) were placed in a non-woven bag. The bag was packed up and immersed in deionized water under various temperatures which were controlled by water bath. When the heating temperature was higher than 100 °C, the packed bag was put in a thermal aging cell filling with 100 mL deionized water. Subsequently the thermal aging cell was sealed and put in an oven. Once the BSP contacting with deionized water, the evolution of the weight of bag was recorded after specific time intervals. The bag was carefully removed and drained excess water for 3 min. After weighing the bag was put into deionized water again for continuous water absorption under a certain temperature. The swelling rate (g/g) was obtained according to the following equation [16]:

$$S = \frac{m_t}{m_0} * 100\% \quad (1)$$

Where, S is the swelling rate,  $m_t$  is the weight of BSP after a period of time,  $m_0$  is the initial weight of BSP.

### 2.4. Zeta potential and particle size distribution measurement

Bentonite (16.0 g) and sodium carbonate (0.8 g) were added into 400 mL deionized water and stirred at 10000 rpm for 30 min. Then the suspension was sealed and incubated at ambient temperature for 24 h to achieve complete hydration. The prepared bentonite suspension is also called bentonite-based drilling fluid with pH value of 9.8. The BSPs with different concentrations were mixed into the hydrated bentonite suspension separately by stirring at 8000 rpm for 20 min. In order to investigate the influence of inorganic salts on the rheological and filtration properties of bentonite suspension containing BSPs, NaCl and CaCl<sub>2</sub> with varying concentrations were added into the bentonite suspension containing 1.0 w/v% BSPs respectively by stirring at 8000 rpm for 20 min.

For colloid particles, when dispersing in the aqueous solution, the surface charge at the interface of the droplets can be determined by zeta potential [17]. The zeta potential of the particles was measured with a multi-angle granularity and zeta potential analyzer (NanoBrook Omni, Brookhaven Instruments) using phase-analysis light scattering. Prior to measurement, the suspension was diluted to assure the particles visible under the microscope. Three duplicated tests were performed at 20 °C. The particle size distribution of the particles was measured using a Bettersize 2000 laser particle size analyzer (Bettersize instruments Ltd., China).

### 2.5. Rheological and filtration measurement of bentonite suspension

In order to evaluate the high temperature stability, the drilling fluids prepared in section 2.4 were hot rolled in an oven at a setting temperature for 16 h [1]. By comparing the rheological and filtration properties of the drilling fluid measured before hot rolling

(BHR) and after hot rolling (AHR), the high temperature stability could be judged. The rheological measurements were conducted using a model ZNN-D6 six-speed rotating viscometer (Qingdao Haitongda Special Instrument Co., Ltd., China) according to the API standard. The rheological parameters including apparent viscosity (AV), plastic viscosity (PV) and yield point (YP) were obtained based on the following equations [18]:

$$\text{Apparent viscosity (AV)} = \Phi 600/2 \text{ (mPa s)} \quad (2)$$

$$\text{Plastic viscosity (PV)} = \Phi 600 - \Phi 300 \text{ (mPa s)} \quad (3)$$

$$\text{Yield point (YP)} = (\Phi 300 - \text{PV})/2 \text{ (Pa)} \quad (4)$$

Where  $\Phi 600$  and  $\Phi 300$  are the dial readings at 600 and 300 rpm, respectively.

The API filtration tests were performed using a ZNZ-D3-type medium-pressure filtration apparatus (Qingdao Haitongda Special Instrument Co., Ltd., China). The pressure difference was set to be 0.7 MPa and the test was lasted for 30 min using a filter paper as filter medium [18]. The filter cake thickness was measured with a vernier caliper. After the test, the appearance of the fresh filter cake was recorded by photography. Then shock-freezing in liquid nitrogen and freeze drying at  $-50\text{ }^{\circ}\text{C}$  were used in succession to dry the filter cake, which was capable of removing the free water and adsorbed water in the filter cake by sublimation, and in turn maintained the original morphology of the filter cake [19]. The structure of the dried filter cakes were analyzed by a scanning electron microscope (SEM, Sigma300, Zeiss).

### 3. Results and discussion

#### 3.1. Effect of BSPs on the rheological properties of bentonite suspension

##### 3.1.1. Effect of temperature

As shown in Fig. 1, prior to hot rolling, the rheological parameters including AV, PV, and YP increased progressively with the increasing concentration of BSPs. At BSP concentrations below 1.0 w/v%, the variation of the rheological parameters (AV, PV and YP) is almost linear with the BSP concentration with a lower slope. For BSP concentration above 1.0 w/v%, the rheological parameters increased sharply with a higher slope. When the BSP concentration was 3.0 w/v%, an unacceptable high viscosity was observed which probably did not favor drilling.

By comparing the rheological parameters prior to and after thermal aging at various temperatures, it is possible to assess the temperature stability of the fluid [20]. It was found that after hot rolling at  $90\text{ }^{\circ}\text{C}$ , AV, PV and YP demonstrated close values to that of before hot rolling, suggesting a thermal stable fluid. When the hot rolling temperature was  $120\text{ }^{\circ}\text{C}$ , the rheological parameters after hot rolling exhibited decline to a certain extent. As the thermal aging temperature was further increased to  $150\text{ }^{\circ}\text{C}$ , all the rheological parameters exhibited a remarkable decline at all the concentration range. The molecular conformation transition and molecular chain degradation induced by such high temperature in basil seed gum probably explained this phenomenon [21]. Meanwhile, it could be seen that the BSPs are tolerant to  $120\text{ }^{\circ}\text{C}$ .

Generally, the pH value of drilling fluid is adjusted to be alkaline. Since the particle association between Na-montmorillonite platelets is pH dependent, a face-to-face connection takes place at such pH values [22]. While for BSP, the carboxyl groups in basil seed gum dissociate and the molecular conformation changes from a compact coil or sphere at low pH value to a stretched chain at alkaline environment, which favors the increase of the

hydrodynamic size of the polysaccharides. Meanwhile at low concentration of dilute suspension, the polysaccharide molecules in BSP can move freely and be adsorbed onto the clay particles surface. While at high concentrations, a saturated adsorption was obtained. The mutual contact of polysaccharide molecules start to occur, which restricted their movement. The change from free moving molecules to an entangled network results in the viscosity increment [23]. In addition, the more complex branching in basil seed gum compared with conventional linear polysaccharides correlates with an efficient gelation capacity [24]. These probably explained that the viscosity increased with a higher slope when the BSP concentration above 1.0 w/v%. The great influence of BSP on the rheological properties of bentonite suspension at high concentration indicated that the macroscopic behavior of the basil/bentonite mixtures is predominantly controlled by basil [25].

Basil seed gum solutions exhibited shear thinning and thixotropic behavior [12,26–28]. The basil seed gum also forms a weak gel like many polysaccharide gums [15]. From a practical point of view, these characteristics allow the drilling fluid to be pumped easily and are desirable for hole cleaning operations in drilling as they provide a high level of carrying capacity for the mud solid particles and the drilled cuttings [12,29]. In terms of filtration control, an increased viscosity of filtrate corresponded to a lower filtration loss rate according to the Darcy law.

The images of bentonite suspension containing varying concentrations of BSPs are given in Fig. 2. At 2.0 w/v% and 3.0 w/v% BSP, the system changed from a high viscous flowing suspension to a consolidated self-supporting hydrogel structure under gravitational force [30], which is consistent with that of rheological testing results.

##### 3.1.2. Effect of inorganic salts

Since the high salinity formations are typically encountered in drilling, the tolerance of a polymer towards salts pollution such as  $\text{Na}^+$  and  $\text{Ca}^{2+}$  is an especially valuable property [31]. The effect of NaCl and  $\text{CaCl}_2$  on the rheological properties of bentonite suspension with 1.0 w/v% BSP before and after thermal aging at  $120\text{ }^{\circ}\text{C}$  was studied respectively.

As shown in Fig. 3, regardless of thermal aging, the rheological parameters including AV and PV decreased sharply when the NaCl concentration was lower than about 3.0 w/v%, then followed by a relatively slight change until the NaCl concentration reaching up to 15.0 w/v%. In the case of YP, for the pristine bentonite suspension, it decreased with the increasing concentration of NaCl and then kept slight change before hot rolling, while varied slightly from 1 Pa to 1.5 Pa after hot rolling. For the bentonite suspension containing BSPs, the YP followed the same trend that it decreased rapidly initially and then change little when the NaCl concentration above 3.0 w/v%. For the divalent salt of  $\text{CaCl}_2$ , as shown in Fig. 4, a similar trend for the variation of the rheological parameters with  $\text{CaCl}_2$  concentration was also observed. However,  $\text{CaCl}_2$  imparted a more significant influence.

For the Na-bent suspension, the diffuse double layer of the bentonite platelets would be compressed by the cationic ions of the salts and result in aggregation of bentonite platelets, meanwhile, as the temperature increase, the bentonite particles are more prone to flocculation with the existence of electrolyte like NaCl, which consequently decreased the viscosity of the bentonite suspension [32,33]. While for the Na-bent/BSP suspension, the  $\text{Na}^+$  ions would neutralize the carboxyl groups along the polymer chains, which weakens the repulsion between adjacent chains and allows closer association, causing a significant reduction in viscosity [12,34]. As a divalent salt,  $\text{CaCl}_2$  has a larger hydrated radius than NaCl, implying that  $\text{Ca}^{2+}$  ions exert more intense electrostatic shielding interaction between polymer chains than  $\text{Na}^+$  ions, therefore decrease the

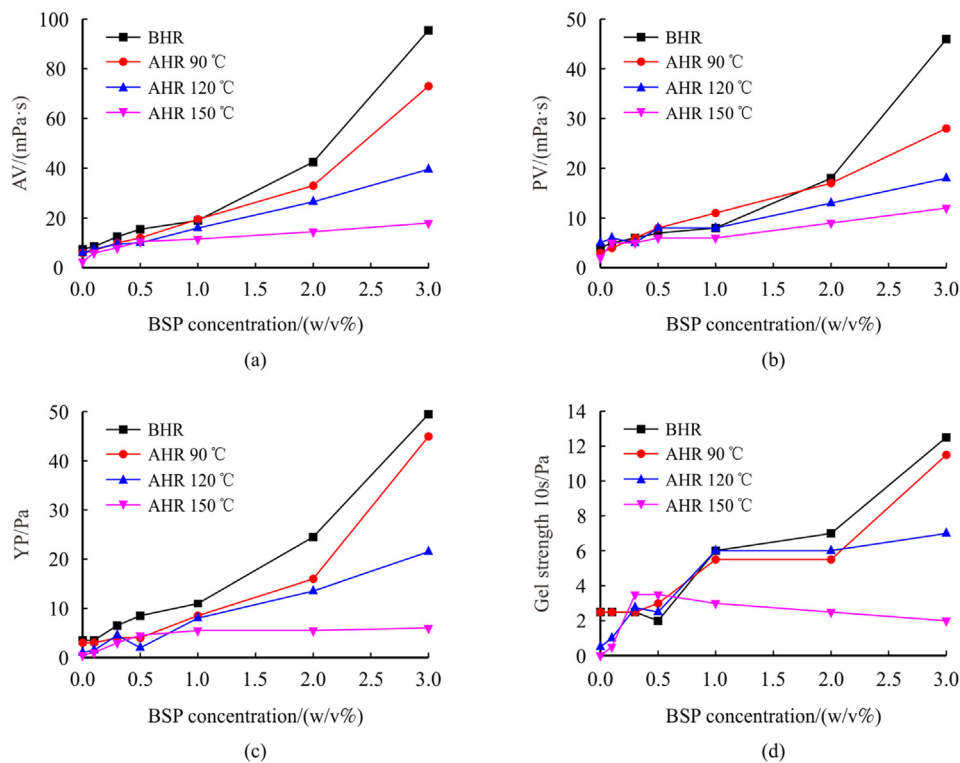


Fig. 1. Rheological properties of BSP suspension at various concentrations.

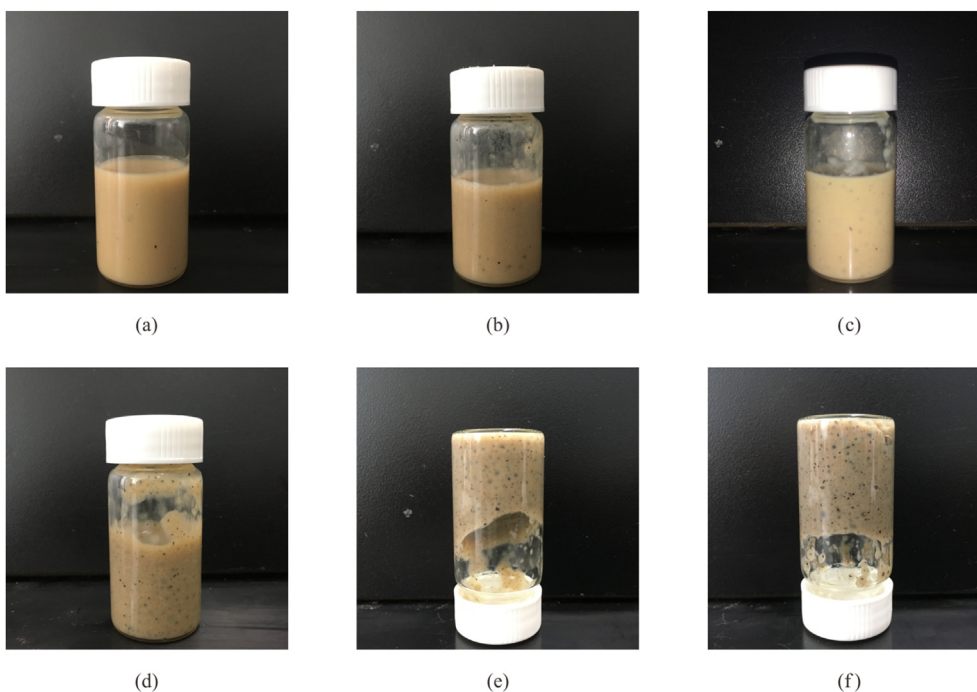


Fig. 2. Images of the BSP-Na-bent hydrogels. (Note: a: 0.1 w/v% BSPs; b: 0.3 w/v% BSPs; c: 0.5 w/v% BSPs; d: 1.0 w/v% BSPs; e: 2.0 w/v% BSPs; f: 3.0 w/v% BSPs).

polymer expansion and repulsion more obviously, and in turn affect more on viscosity [34].

### 3.2. Effect of BSPs on the filtration properties of bentonite suspension

#### 3.2.1. Effect of temperature

BSPs were mixed into the bentonite suspension and hot rolled at different temperatures. The evolution of API filtration loss volume

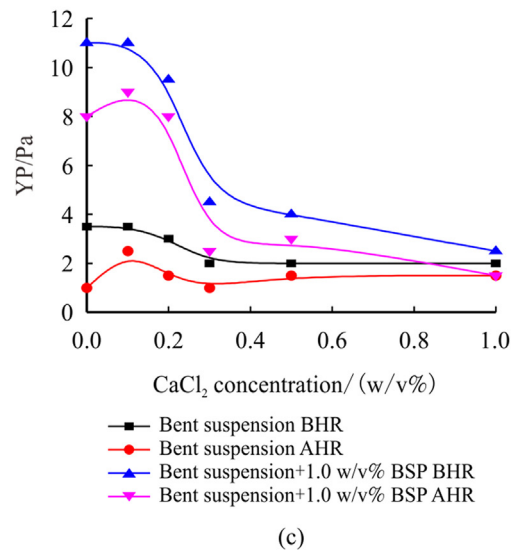
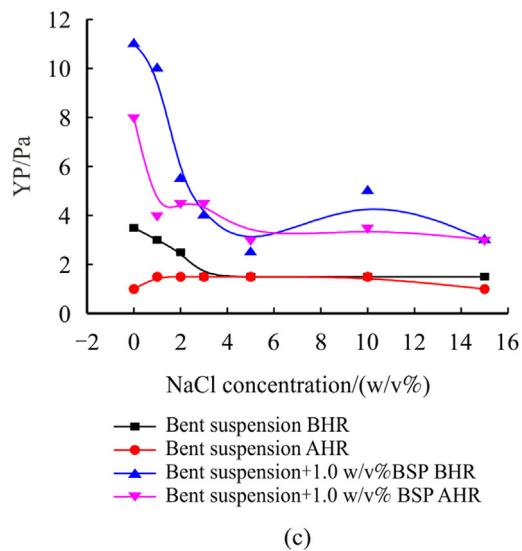
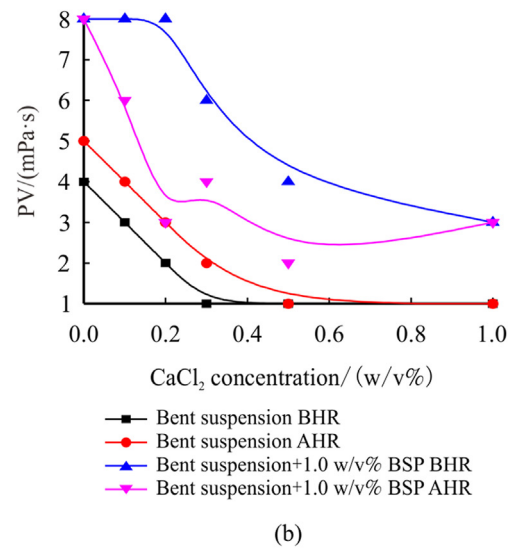
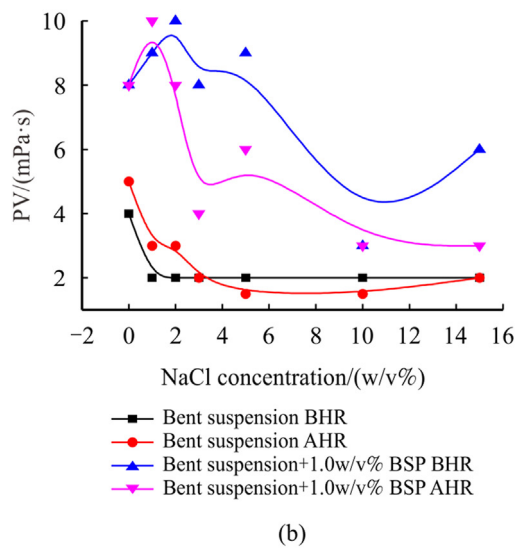
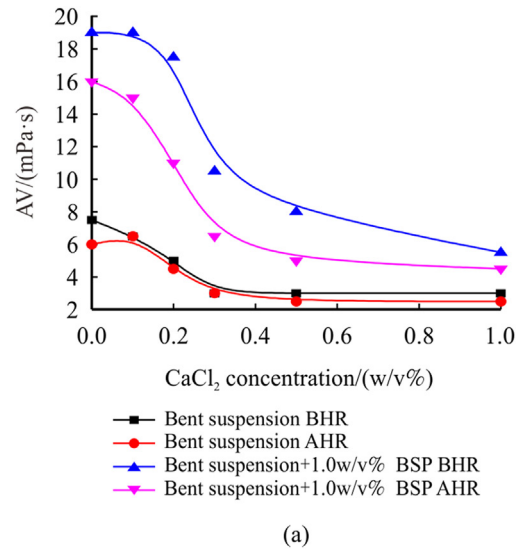
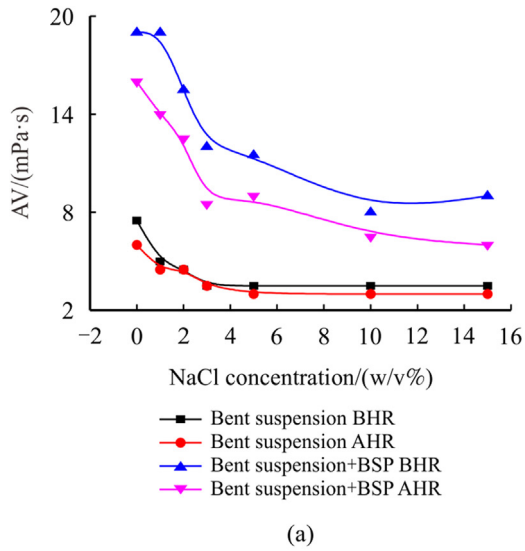


Fig. 3. Influence of NaCl on the rheological properties of bentonite suspension containing 1.0 w/v% BSPs before and after hot rolling at 120 °C.

Fig. 4. Influence of CaCl<sub>2</sub> on the rheological properties of bentonite suspension containing 1.0 w/v% BSPs before and after hot rolling at 120 °C.

of the suspension with testing time is illustrated in Fig. 5. For the initially a few minutes, the filtration loss rate was high for all the suspensions because of the absence of forming thin filter cake. As the filtration experiment continued, the filtration loss rate declined due to the gradual formation of the filter cake [33]. It is shown that as the BSP concentration increased, the high filtration rate stage gradually decreased from about 5 min to 3 min, indicating an enhanced filtration control. After forming the filter cake, the filtration loss rate seen from the slope of the filtration curve also decreased gradually with the increase of the BSP concentration, indicative of effective filtration control.

The evolution of filtration loss volume and filter cake thickness with BSP concentration before and after hot rolling at different temperatures were depicted in Table 1. It is seen from Table 1, the filtrate volume decreased sharply at low BSP concentrations and then changed slightly at concentration above 1.0 w/v%. Meanwhile, although thermal aging at 90 °C and 120 °C exerted a certain degree of influence on the viscosity of the bentonite suspension in the presence of BSPs, the filtration volume before and after hot rolling at 90 °C and 120 °C displayed relatively slight change, suggesting that BSPs are capable of controlling the filtration loss under such temperatures. However, when the hot rolling temperature increased to 150 °C, the filtration loss curve was translated upward remarkably in the whole range of BSP concentration, showing a less effective filtration control. For one hand, the aggregation of clay particles at high temperature resulted in less efficiency of forming dense filter cake [35]. For the other hand, the degradation of basil seed gum under such high temperature may take more responsibility. The degradation of basil seed gum and the flocculation of clay particles may also explained the increased thickness of filter cake [36]. Prior to thermal aging, the thickness of filter cake decreased rapidly and then gently as the BSP concentration increased. After hot rolling at 90 and 120 °C, it exhibited a similar trend, which was in agreement with the filtration loss volume change. Whereas, after hot rolling at 150 °C, the thickness of the

filter cake decreased firstly and increased again at BSP concentration above 0.3 w/v%.

The variation of filter cake appearance with the concentration of BSP before and after hot rolling at various temperatures is shown in Fig. 6. Prior to hot rolling, the filter cake became smooth and thin since more and more BSPs took part into the establishment of filter cake. At the same time, the filter cake gradually exhibited darker with the increase of thermal aging temperature, which was ascribed from the gradual degradation of basil seed.

### 3.2.2. Effect of inorganic salts

The influence of inorganic salts (NaCl and CaCl<sub>2</sub>) on the filtration properties of bentonite suspension having 1.0 w/v% BSPs is shown in Fig. 7 and Fig. 8. The Na<sup>+</sup> ions compress the diffuse double electric layer of the bentonite platelets, resulting in the releasing of adsorbed water and flocculation of bentonite platelets [33]. Therefore, the bentonite particles mainly associated with face-to-face style and cannot form compact filter cake. For bentonite suspension added with 15.0 w/v% NaCl, the filtration loss volume increased from 26.8 mL to 105.6 mL (Fig. 7a). After hot rolling at 120 °C, the filtration loss further increased to 166 mL because of the aggregation of bentonite particles under high temperature environment [32]. However, after adding 1.0 w/v% BSPs, the filtration loss increased slightly from 11.4 mL to 16 mL, and 13.7 mL–38.6 mL before and after hot rolling, respectively. It is also shown in Fig. 7b that there was a relatively small difference for the filtration reduction rate before and after thermal aging for NaCl concentration below 5.0 w/v%, indicating that BSPs possess excellent NaCl tolerance and the filtration loss can be regained through use of BSPs.

Since Ca<sup>2+</sup> ions have stronger probability to reduce the repulsion than Na<sup>+</sup> ions, the CaCl<sub>2</sub> has more influence on the filtration. Meanwhile, larger cations (Ca<sup>2+</sup>) exhibited stronger electrostatic shielding interaction between basil seed gum chains than small cations [34]. When only 1.0 w/v% CaCl<sub>2</sub> was incorporated, the

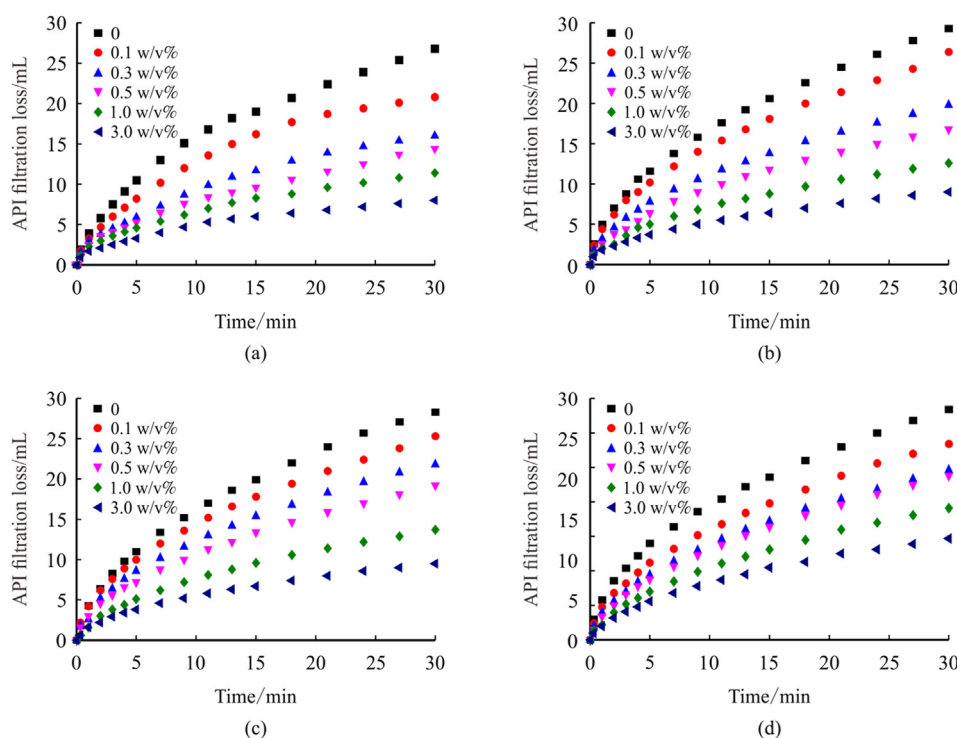


Fig. 5. Variation of API filtration loss with time. Note: (a) BHR; (b) AHR at 90 °C; (c) AHR at 120 °C; (d) AHR at 150 °C.

**Table 1**  
API filtration loss and filter cake thickness as a function of BSP concentration before and after hot rolling at different temperatures.

BSP concentration (w/v%)	API filtration loss (mL)				Filter cake thickness (mm)			
	BHR	AHR 120 °C	AHR 120 °C	AHR 150 °C	BHR	AHR 120 °C	AHR 120 °C	AHR 150 °C
0	26.8	29.3	28.3	33.4	2.8	2	2.1	1.6
0.1	20.8	26.4	25.3	28.4	2.4	2	2	1.5
0.3	16	19.8	21.8	24.6	2	1.8	1.6	1.4
0.5	14.4	16.8	19.2	23.8	1.7	1.5	1.5	1.5
1	11.4	12.6	13.7	19.1	1.56	1.2	1.4	1.8
3	11	9	9.5	14.7	1.58	1.1	1.5	2.1

filtration loss of the bentonite suspension reached as high as 95 and 116 mL respectively, before and after hot rolling (Fig. 8a). For the bentonite suspension containing 1.0 w/v% BSP, the filtration loss only raised from 11.4 mL to 19.6 mL, indicating that CaCl<sub>2</sub> has little impact on the filtration loss of the system before hot rolling. However, the filtration loss also increased obviously after hot rolling at 120 °C. From Fig. 8b, the filtration reduction rate declined sharply when the CaCl<sub>2</sub> above 0.3 w/v%. Therefore, the bentonite suspension with 1.0 w/v% BSP can resist 0.3 w/v% CaCl<sub>2</sub> pollution under 120 °C.

### 3.3. Filtration controlling mechanism

#### 3.3.1. Water absorbency capacity of BSPs

The water absorption behavior of BSPs under various temperatures is depicted in Fig. 9. The water absorption rate increased speedily at the initial half hours, followed by slight increase with testing time. Meanwhile, the water absorption rate decreased as the testing temperature increased. The water absorption rate started to decrease after testing for 4 h and 2 h when testing at 120 °C and 150 °C, respectively. This was probably attributed to the fact that the polysaccharides in the BSPs started to degrade under such high temperatures. After the test the suspension became tawny, which also confirmed the partial degradation of the BSPs. The high water retention capacity contributed to the gelatious structure and viscosity increment, which influences on their rheological properties and filtration control.

The polarized microscope photographs of the BSP in deionized water are presented in Fig. 10. As depicted in Fig. 10a, a large amount of fascicular villus stretched from the outer surface of the basil seed into the aqueous solution, which provides a huge specific surface area for water absorption. In addition to the fluffy fiber bundles, considerable nearly spherical particles ranging from 5 to 10 μm were also observed in Fig. 10b, which could effectively plug the micro pores of filter cake and reduce filtration loss.

The morphologies of the basil seed gum after freeze-dried were examined by SEM and presented in Fig. 11. As depicted in Fig. 11a, bundles of fibril structures and globular structures were connected mutually to form three dimensional (3D) networks. A magnified picture in Fig. 11b further confirmed that a nanoscale 3D network was fabricated for the basil seed gum in aqueous solution. Samateh et al. [24] reported a similar structure and explained that complicated branching in basil results in this nanoscale 3D network and effective gelation ability.

The highly porous nature of the basil seed gum provides an easy channel to water which is necessary for rapid and high swelling [16,37]. Since there are plentiful hydroxyl groups and branched units in the polysaccharides of basil seed, the entanglement of the polysaccharide chains and formation of hydrogen bonds from the intra- and inter-molecular polysaccharides and water would result in water absorption and swelling [14,24,38]. It should be noted that the striking water absorption would decrease the free water

content of the drilling fluid and minimize the filtration loss. Furthermore, the polysaccharides after water absorption would form hydration layer and the macromolecular chains become more elastic, which are beneficial for forming a more compressible filter cake and in turn decreasing the filtration.

#### 3.3.2. Zeta potential measurement

As shown in Fig. 12a, the BSP suspensions of all the concentrations have negative zeta potential ranging from -27.6 to -40.3 mV, which could be attributed to the anionic character of basil seed gum [39]. As the BSPs concentration increased, the absolute value of zeta potential increased probably due to the increased repulsion arising from the carboxyl groups of basil seed gum. As the concentration reached to 0.3 w/v%, the zeta potential began to decrease and then changed slightly. The increased concentration of BSPs resulted in increased viscosity and less mobility in comparison with small particles, which contributed to the decrement of zeta potential [40].

As depicted in Fig. 12b, the influence of BSPs on the zeta potential of bentonite suspensions displayed a similar tendency. Although the basil seed gum is anionic, the adsorption of the polysaccharides in the BSP on the bentonite particle surface can occur via several interactions including anionic ionic exchange, hydrogen bonding and electrostatic bridging by intermediated cations like other anionic polymers [25,41]. Generally a higher absolute value of zeta potential indicates a more stable particle suspension. The adsorption of basil seed gums contributed to the more negative zeta potential and led to steric stabilization of fine particles, which plays a vital role in forming dense filter cake and reducing the filtrate invasion.

The effect of NaCl and CaCl<sub>2</sub> on the zeta potential of bentonite suspension with and without BSPs is presented in Fig. 12c and d. In the absence of BSPs, the monovalent salt NaCl affected the zeta potential of bentonite suspension by a limited degree as seen from the gentle variation of zeta potential with increasing concentration of NaCl. While divalent salt CaCl<sub>2</sub> exhibited a remarkable effect by compressing the thickness of diffused electric double layer [42]. After incorporating of 1.0 w/v% BSPs, the zeta potential decreased speedily at low concentrations of NaCl and then kept gentle change. While for CaCl<sub>2</sub>, the zeta potential decreased gradually with the increasing concentration of CaCl<sub>2</sub>. When the concentration of NaCl and CaCl<sub>2</sub> are lower than 5.0 w/v% and 0.3 w/v% respectively, the addition of BSPs generated higher absolute values of zeta potential compared to that of bentonite suspensions alone, suggesting that addition of BSPs improves the suspension stability, which explained the effective filtration control under such salts environment.

#### 3.3.3. Particle size distribution measurement

The effect of BSPs on the particle size distribution of bentonite suspension before and after hot rolling at various temperatures is given in Fig. 13. The shift of particle size distribution exhibited a similar trend for all suspensions regardless of thermal aging. When

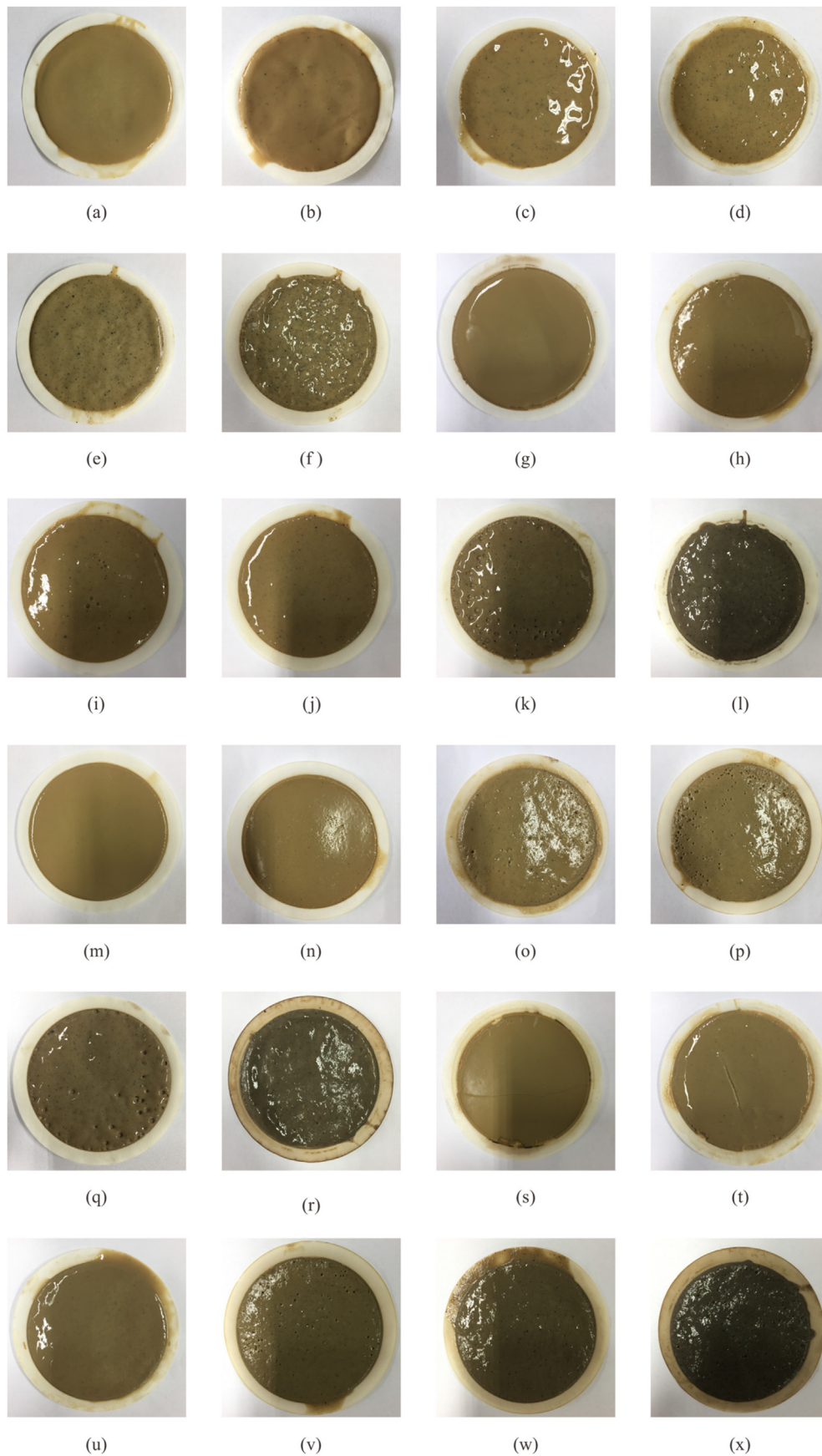


**Fig. 6.** The variation of API filtration cake appearance with thermal aging temperatures in the presence of BSPs. Note: a: BHR, b: AHR at 90 °C; c: AHR at 120 °C; d: AHR at 150 °C. 1: control sample; 2: 0.1 w/v%; 3: 0.3 w/v%; 4: 0.5 w/v%; 5: 1.0 w/v%; 6: 3.0 w/v%.

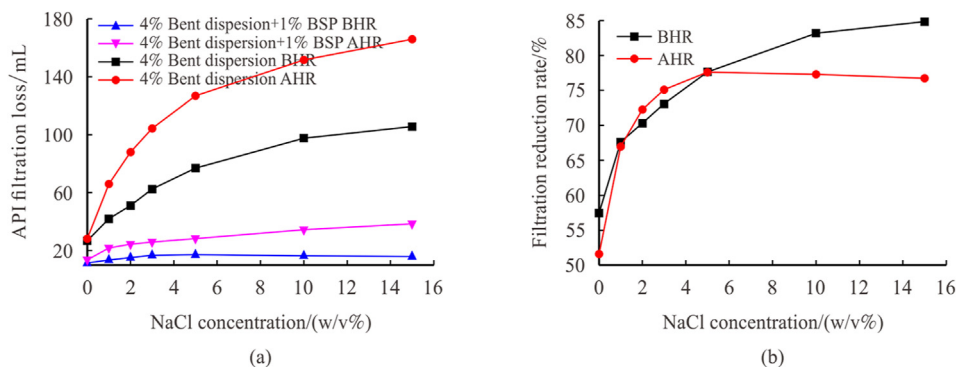


Fig. 7. Variation of API filtration loss (a) and filtration reduction rate (b) with NaCl concentration before and after thermal aging at 120 °C.

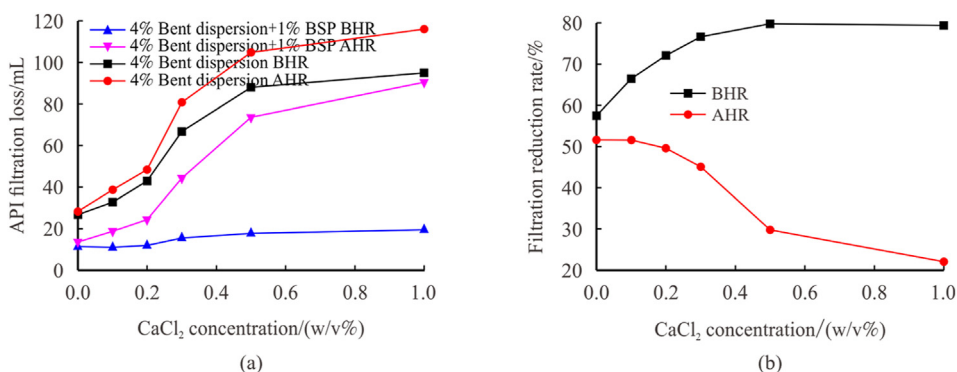


Fig. 8. Variation of API filtration loss (a) and filtration reduction rate (b) with calcium chloride concentration before and after thermal aging at 120 °C.

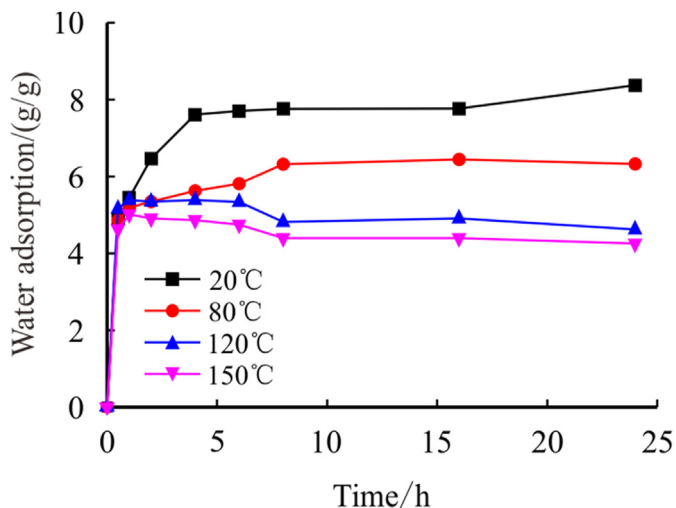


Fig. 9. Variation of Water adsorption rate of BSPs with time under various temperatures.

BSPs with low concentration was first added to the bentonite suspension, the particle size distribution displayed slight variation. Subsequent addition of 2.0 w/v% BSPs caused a rapid size increase due to the aggregation occurrence. This was also observed for the evolution of median size (D50) with BSP concentration (Fig. 14a). At low BSP concentration, the polysaccharides in the basil seed gum would be adsorbed onto the bentonite particle surface, which prevented the agglomeration and led to the steric stabilization of bentonite particles due to the strong electrostatic repulsions of

anionic side chains. Meanwhile, the high charge density side chains formed very rigid conformation, which was not favorable for bridging [25,42]. While at high concentrations (above 1.0 w/v%), the physical or chemical interactions between polysaccharide molecules and bentonite particles were enhanced so that the larger and stronger aggregation developed. This was also observed from the BSP suspension itself (Fig. 14b), that as the concentration increased, the median particle size (D50) increased slightly, but abruptly at critical aggregation concentration of 1.0 w/v%.

### 3.3.4. Microstructure of filter cake

The SEM images of API filtration filter cake for the bentonite suspension before and after thermal aging at 120 °C was shown in Fig. 15. For the bentonite suspension prior to thermal aging, the clay particles attach themselves with edge-to-face arrangement and formed a gel structure (Fig. 15a) [43]. The aggregation of the clay particles in some degree led to the formation of a heterogeneous structure having irregular pores, which offered a facilitated filtration passage and generated an unacceptable filtration loss. As shown in Fig. 15b, the incorporation of 1.0 w/v% BSPs generated a typical honeycomb structure like other polymers [44]. Numerous far-reaching filaments bridged with the pores of the filter cake like “fingers”. These polymer chains formed bridging structures between the bentonite platelets and extended into the pore space where the filtrate has to pass through [31,45]. Meanwhile, the highly porous 3D network with numerous fibril and globular structures of basil seed gum provides enough space to entrap water filtration. Therefore, although numerous pores were observed in Fig. 15b, these pores were actually filled with a large amount of trapped water before freeze-drying. After thermal aging, the elevated temperature induced the dehydration of clay particles,

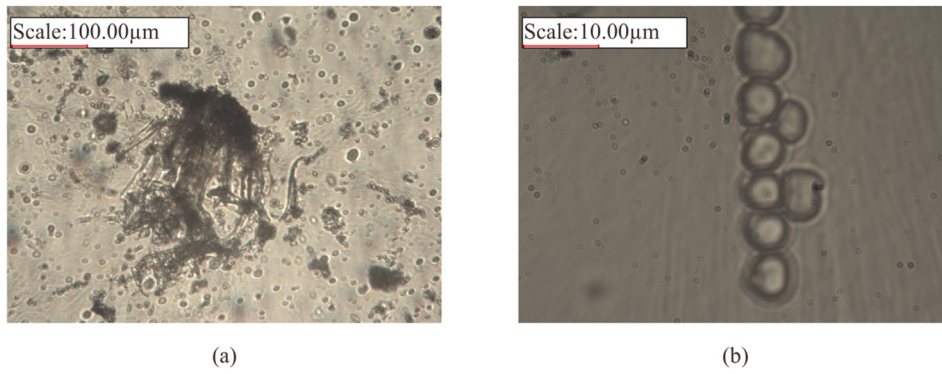


Fig. 10. Polarizing microscope photographs of BSP suspension.

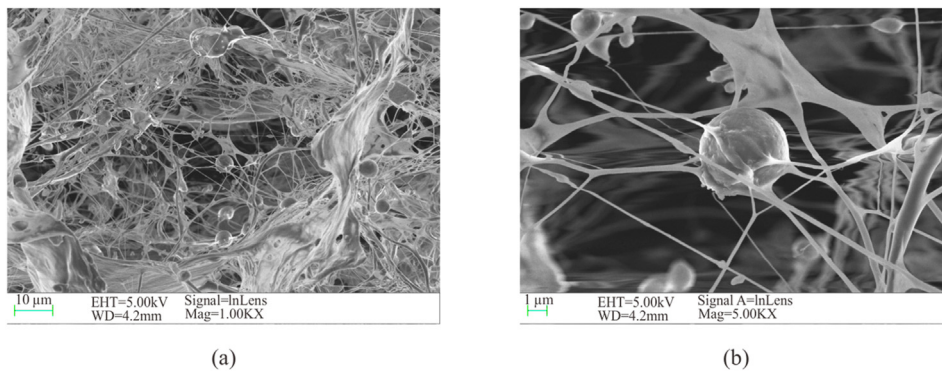


Fig. 11. SEM photographs of 0.5 w/v% BSP suspension.

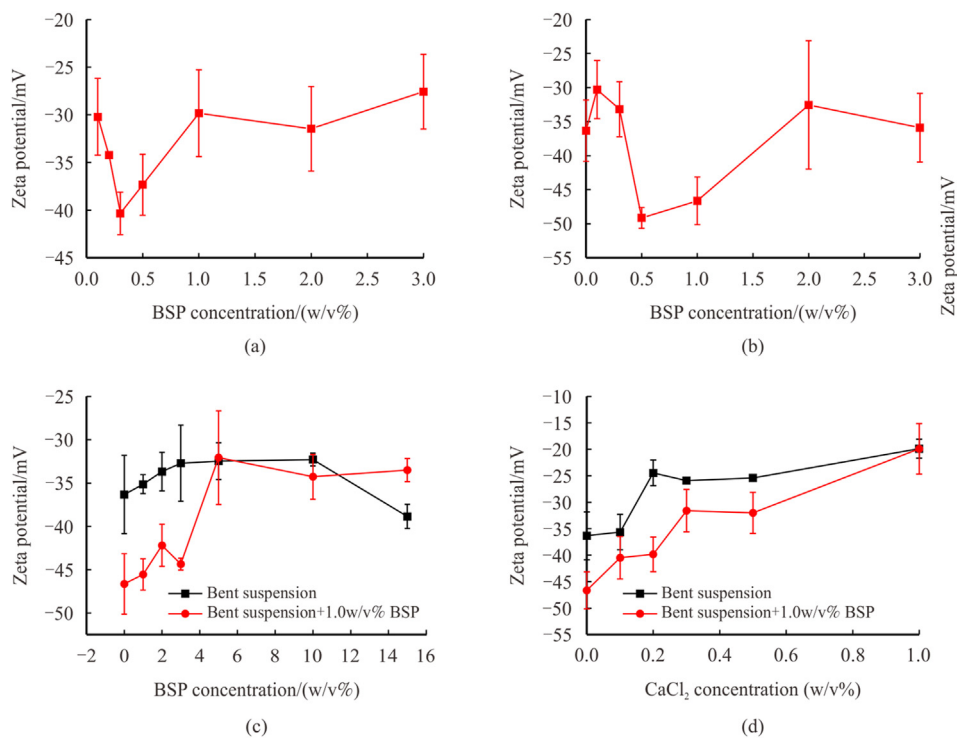


Fig. 12. The zeta potential measurement results of various suspensions. Note: a: BSP suspension; b: bentonite suspension with varying BSP concentrations; c: bentonite suspension with NaCl of varying concentrations; d: bentonite suspension with CaCl<sub>2</sub> of varying concentrations.

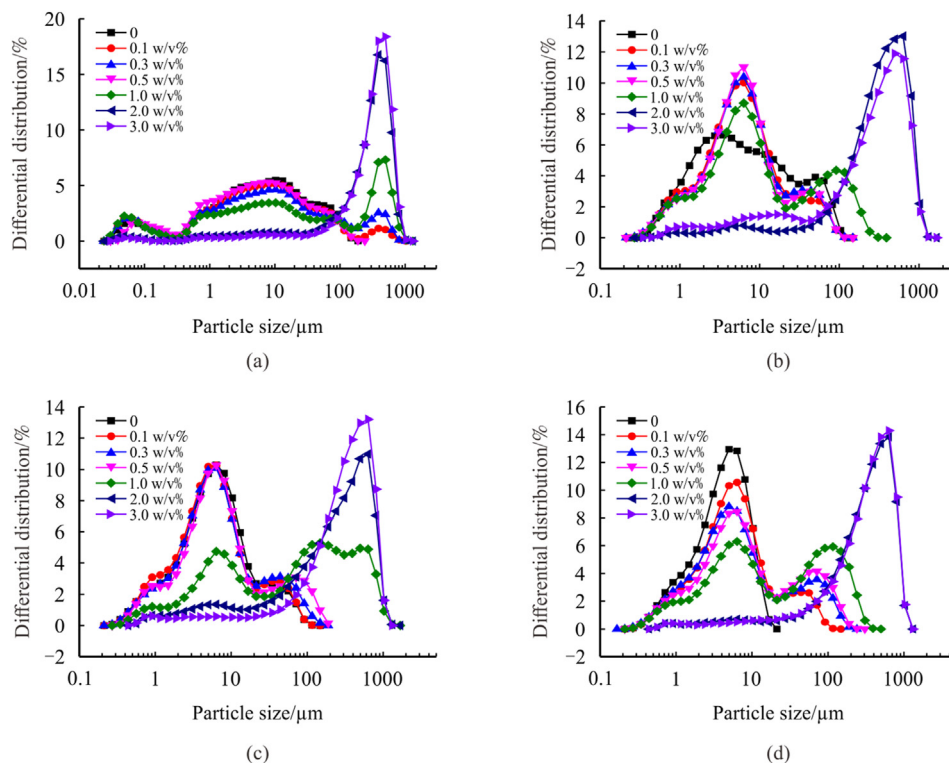


Fig. 13. The variation of medium particle size of bentonite suspension with BSP concentration after thermal aging. Note: a: BHR; b: AHR at 90 °C; c: AHR at 120 °C; d: AHR at 150 °C.

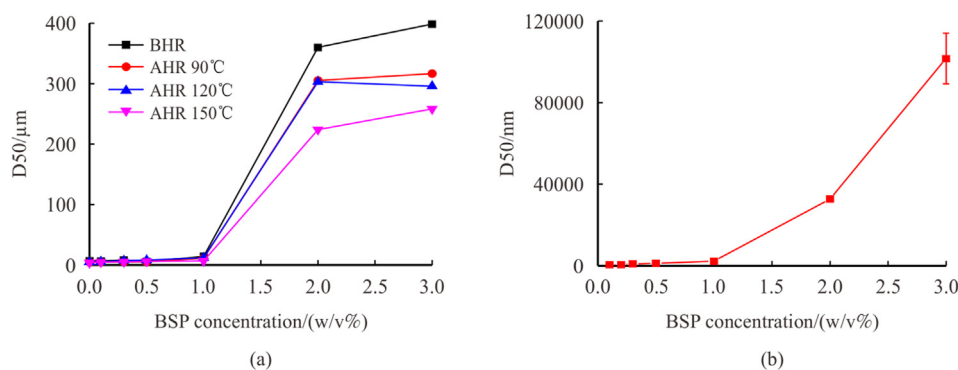


Fig. 14. Variation of medium particle size for (a) bentonite suspension and (b) BSP suspension with BSP concentration.

therefore, more and more bentonite particles tended to form face-to-face arrangements, which provided an enlarged filtration channel and less efficient filtration control (Fig. 15c). While for the suspension with BSPs, as depicted in Fig. 15d, although this high temperature induced degradation of BSP in some degree, the typical honeycomb structure and polymer fingers still existed, indicating the effective filtration control.

As shown in Fig. 16a, for the bentonite suspension with 10.0 w/v % NaCl, the bentonite particles aggregated and formed large particles, which left relatively large pores and lost control of filtration. Meanwhile, small square crystals of NaCl were also observed by mixing with bentonite particles. After addition of 1.0 w/v% BSP, as depicted in Fig. 16b, bundles of rod-like NaCl crystals were stacked together with bentonite particles and formed a denser filter cake. The electrostatic adsorption between anionic basil seed gum and  $\text{Na}^+$  probably prompted these growth of crystals. The divalent  $\text{Ca}^{2+}$  ions had a more profound influence on the structure of bentonite

suspension. After adding 0.5 w/v%  $\text{CaCl}_2$  into the bentonite suspension, there were a large number of pores formed by flocculation of bentonite particles (Fig. 16c), also suggesting the losing of filtration control. Whereas, the incorporation of BSPs exhibited a totally different appearance. It could be seen from Fig. 16d, the relatively small bentonite particles aggregated together to form a denser filter cake. Furthermore, the fibril structure coming from BSPs was also observed to embed into the filter cake. Thereby, the addition of BSP into bentonite suspension prevented the flocculation of bentonite particles under the high electrolyte environment, which drastically enhanced the filtration control capacity.

### 3.3.5. Filtration control mechanism analysis

Numerous studies have been reported concerning the filtration control with anionic polymers. Generally the anionic polymers decrease the filtration loss by reducing the free water content of the drilling fluid, viscosifying and slowing down the filtration rate,

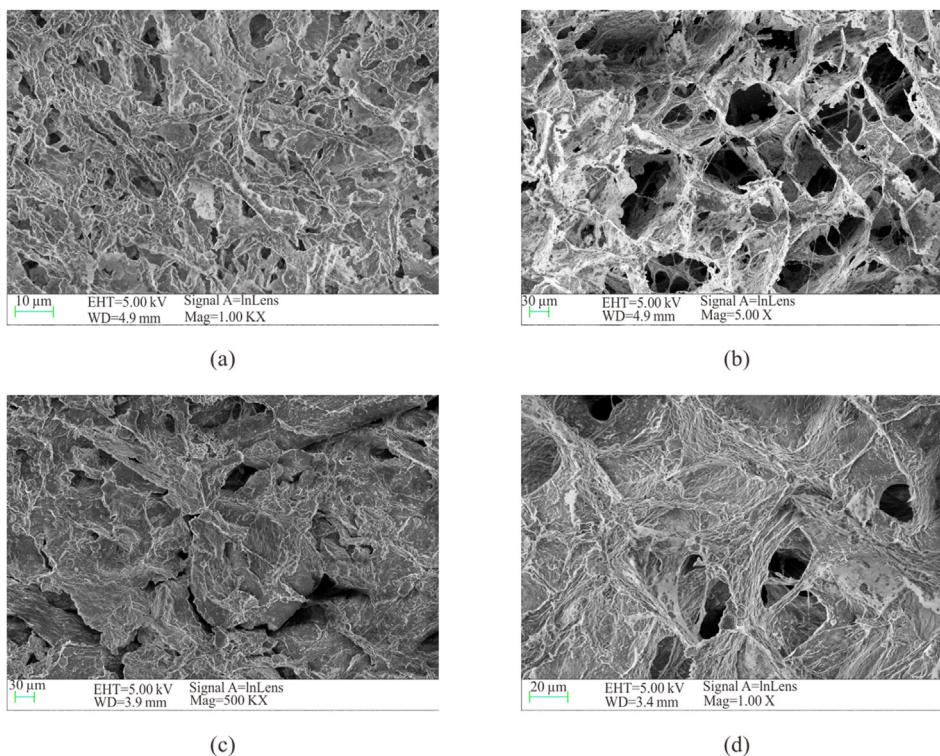


**Fig. 15.** SEM photographs of filter cakes before and after thermal aging at 120 °C. Note: (a) Bentonite suspension BHR; (b) Bentonite suspension with 1.0 w/v% BSP BHR; (c) Bentonite suspension AHR; (d) Bentonite suspension with 1.0 w/v% BSP AHR.

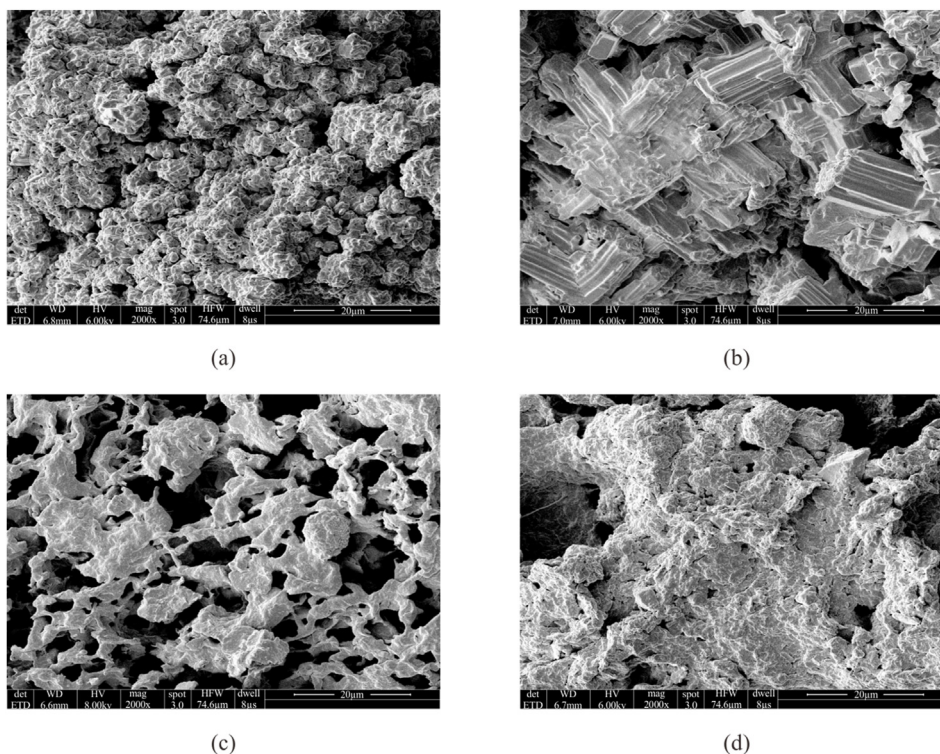


**Fig. 16.** SEM images of API filtration filter cake for bentonite suspension contaminated with inorganic salts before and after BSP incorporation. Note: a: bentonite suspension +10.0 w/v% NaCl; b: bentonite suspension +1.0 w/v% BSPs +10.0 w/v% NaCl; c: bentonite suspension +0.5 w/v% CaCl<sub>2</sub>; d: bentonite suspension +1.0 w/v% BSPs +0.5 w/v% CaCl<sub>2</sub>.

enhancing the dispersion stability of bentonite particles via adsorption, and sealing the micro pores of filter cake with highly

hydrated polymer chains [31–33,46]. In the case of BSPs, the above mechanisms could also be responsible for the observed behavior,

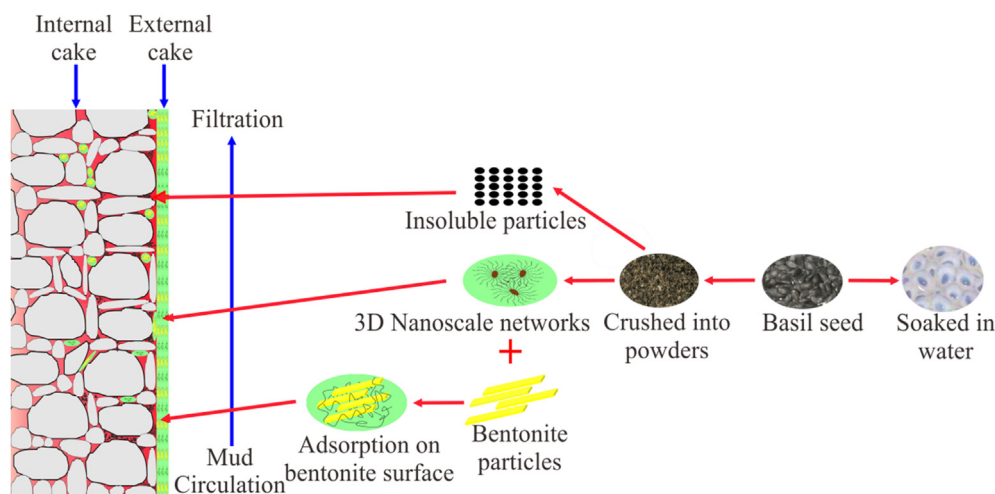


Fig. 17. Scheme of filtration control mechanism of BSPs.

however, some unique characteristics should be emphasized. As seen from Fig. 10b, there were considerable insoluble fine particles in basil seeds, which is critical to filtration control since these fines can effectively fill the micro pores of filter cake [47]. Meanwhile, when dispersed in water, the 3D nanoscale networks with numerous fibril and globular particles formed the inherent hierarchical micro/nano structures, which offer excellent fabric and favorable space for water absorption [48]. For the one hand, these networks can take part into forming the filter cake in combination with bentonite particles, which reduce the permeability of filter cake. For the other hand, their extraordinary water binding capabilities also enable them to directly plug the pores of the filter cake and prevent water passing through with high efficiency, which in turn prevents the filtration loss (Fig. 17) [31].

In regard to electrolytes contamination, the presence of  $\text{Na}^+$  and  $\text{Ca}^{2+}$  promoted the adsorption of anionic polysaccharide polymers onto the surface of bentonite particles [49]. The enhanced adsorption suggested more anionically charged segments were covered on the bentonite particles surface, which prevents the aggregation and flocculation of bentonite particles, thereby results in enhanced stabilization and effective filtration control [32,50].

#### 4. Conclusions

The addition of BSPs into the bentonite suspension resulted in obvious increase of rheological parameters both before and after hot rolling at 120 °C, but little increase after thermal aging at 150 °C, indicating the inefficiency of BSPs at such temperature due to thermal degradation. With regarding to filtration control, BSPs exhibited very effective filtration control for the bentonite suspension after thermal aging at 90 °C and 120 °C while less efficiency after exposed to 150 °C thermal aging. The bentonite suspension containing 1.0 w/v% BSPs could be tolerant to 5.0 w/v% and 0.3 w/v% sodium and calcium salt pollution respectively with still effective filtration control. Except the general filtration control mechanisms like conventional anionic polymers, the numerous 3D networks that are capable of adsorbing abundant water in combination with considerable small insoluble particles in the basil seed contributed to the excellent filtration control capacity. In the presence of monovalent and divalent salt, the adsorption of basil seed gum onto the bentonite particles generated a shield effect that weakened the flocculation by salts to some extent, which improved the stability and favored the formation of relatively compact filter cake. The outstanding filtration properties of basil seeds endowed they are

green alternatives to traditional synthetic materials in formulating high performance water-based drilling fluids.

#### Credit author statements

Hanyi Zhong: Conceptualization, Methodology, Investigation, Writing-original draft; Xin Gao: Investigation, Writing- review & editing; Xianbin Zhang: Funding acquisition; Anliang Chen: Supervision; Zhengsong Qiu: Investigation, Supervision, Project administration; Xiangzheng Kong: Investigation; Weian Huang: Funding acquisition

#### Declaration of competing interests

The authors declare that they have no known competing financial interests or personal relationships that could have appeared to influence the work reported in this paper.

#### Acknowledgements

This research was supported by CNPC Innovation Foundation (2020D-5007-0310), Natural Science Foundation of China (No. 51974354) and the Fundamental Research Funds for the Central Universities (No.18CX02099A).

#### References

- [1] J. Huo, Z. Peng, Z. Ye, Q. Feng, Y. Zheng, J. Zhang, X. Liu, Investigation of synthesized polymer on the rheological and filtration performance of water-based drilling fluid system, *J. Petrol. Sci. Eng.* 165 (2018) 655–663.
- [2] L. Yang, G. Jiang, Y. Shi, X. Lin, X. Yang, Application of ionic liquid to a high-performance calcium-resistant additive for filtration control of bentonite/water-based drilling fluids, *J. Mater. Sci.* 52 (2017) 6362–6375.
- [3] H.M. Ahmad, M.S. Kamal, M.A. Al-Harhi, High molecular weight copolymer as rheology modifier and fluid loss additive for water-based drilling fluids, *J. Mol. Liq.* 252 (2018) 133–143.
- [4] L.J. Hall, J.P. Deville, C.M. Santos, O.J. Rojas, C.S. Araujo, Nanocellulose and Biopolymer Blends for High-Performance Water-Based Drilling Fluids, SPE-189577-MS, IADC/SPE Drilling Conference and Exhibition, Texas, 2018, 6–8 March.
- [5] Y.M. Wu, B.O. Zhang, T. Wu, C.G. Zhang, Properties of the forpolymer of N-vinylpyrrolidone with itaconic acid, acrylamide and 2-acrylamido-2-methyl-1-propane sulfonic acid as a fluid-loss reducer for drilling fluid at high temperatures, *Colloid Polym. Sci.* 279 (2001) 836–842.
- [6] S. Simon, D.L. Cerf, L. Picton, G. Muller, Adsorption of cellulose derivatives onto montmorillonite: a SEC-MALLS study of molar masses influence, *Colloids Surf., A* 203 (2002) 77–86.
- [7] V.A.V. de Oliveira, K. dos Santos Alves, A.A. da Silva-Junior, R.M. Araújo, R.C. Balaban, L. Hilliou, Testing carrageenans with different chemical

- structures for water-based drilling fluid application, *J. Mol. Liq.* 299 (2020) 1–9.
- [8] S. Kumar, S. Chaurasia, P. Sundriyal, S. Gautam, Synthesis & evaluation of synthesized PAA/AMPS-g-sesbania gum graft copolymer in water based drilling mud system for mitigation of borehole instability in conventional and troublesome formations, SPE-189369-MS, in: SPE/IADC Middle East Drilling Technology Conference and Exhibition, Abu Dhabi, 2018, 29–31 January.
  - [9] R. Mansa, C. Detellier, Preparation and characterization of Guar-montmorillonite nanocomposites, *Materials* 6 (11) (2013) 5199–5216.
  - [10] M.E. Hossain, M. Wajheuddin, The use of grass as an environmentally friendly additive in water-based drilling fluids, *Petrol. Sci.* 13 (2016) 292–303.
  - [11] I. Akbari, S.M. Ghoreishi, Generation of porous structure from basil seed mucilage via supercritical fluid assisted process for biomedical applications, *Int. J. Pharmaceut. Sci. Drug Res.* 3 (1) (2017) 30–35.
  - [12] F. Salehi, M. Kashaninejad, Static rheological study of ocimum basilicum seed gum, *Int. J. Food Eng.* 11 (1) (2015) 97–103.
  - [13] S.M.A. Razavi, S.A. Mortazavi, L. Matia-Merino, A.H. Hosseini-Parvar, A. Motamedzadegan, E. Khanipour, Optimisation study of gum extraction from basil seeds (*Ocimum basilicum* L.), *Int. J. Food Sci. Technol.* 44 (2009) 1755–1762.
  - [14] L. Zhang, Y. Liu, Z. Chen, P. Liu, Behavior and mechanism of ultralow friction of basil seed gel, *Colloids Surf., A* 489 (2016) 454–460.
  - [15] A. Rafe, S.M.A. Razavi, Dynamic viscoelastic study on the gelation of basil seed gum, *Int. J. Food Sci. Technol.* 48 (2013) 556–563.
  - [16] B.A. Lodhi, M.A. Hussain, M. Sher, M.T. Haseeb, M.U. Ashraf, S.Z. Hussain, I. Hussain, S.N.A. Bukhari, Polysaccharide-based superporous, superabsorbent, and stimuli responsive hydrogel from sweet basil: a novel material for sustained drug release, *Adv. Polym. Technol.* (2019) 1–11, 2019.
  - [17] L. Salvia-Trujillo, M.A. Rojas-Grau, R. Soliva-Fortuny, O. Martín-Belloso, Use of antimicrobial nanoemulsions as edible coatings: impact on safety and quality attributes of fresh-cut Fuji apples, *Postharvest Biol. Technol.* 105 (2015) 8–16.
  - [18] H. Zhong, G. Shen, Z. Qiu, Y. Lin, L. Fan, X. Xing, J. Li, Minimizing the HTHP filtration loss of oil-based drilling fluid with swellable polymer microspheres, *J. Petrol. Sci. Eng.* 172 (2019) 411–424.
  - [19] J.P. Plank, F.A. Gossen, Visualization of fluid-loss polymers in drilling-mud filter cakes, *SPE Drill. Eng.* 6 (3) (1991) 203–208.
  - [20] M.A. Tehrani, A. Popplestone, A. Guarneri, S. Carminati, Water-based drilling fluid for HT/HP applications, SPE-105485-MS, in: International Symposium on Oilfield Chemistry, Texas, 2007, 28 February–2 March.
  - [21] C.E. Brunchi, S. Morariu, M. Bercea, Intrinsic viscosity and conformational parameters of xanthan in aqueous solutions: salt addition effect, *Colloids Surf., B* 122 (2014) 512–519.
  - [22] J. Tarchitzky, Y. Chen, Rheology of sodium-montmorillonite suspensions: effects of humic substances and pH, *Soil Sci. Soc. Am. J.* 66 (2) (2002) 406–412.
  - [23] D. Saha, S. Bhattacharya, Hydrocolloids as thickening and gelling agents in food: a critical review, *J. Food Sci. Technol.* 47 (6) (2010) 587–597.
  - [24] M. Samateh, N. Pottachal, S. Manafirasi, A. Vidyasagar, C. Maldarelli, G. John, Unravelling the secret of seed-based gels in water: the nanoscale 3D network formation, *Sci. Rep.* 8 (2018) 1–8.
  - [25] A. Benchabane, K. Bekkour, Effects of anionic additives on the rheological behavior of calcium montmorillonite suspensions, *Rheol. Acta* 45 (2006) 425–434.
  - [26] S.H. Hosseini-Parvar, L. Matia-Merino, K.K.T. Goh, S.M.A. Razavi, S.A. Mortazavi, Steady shear flow behavior of gum extracted from ocimum basilicum L. seed: effect of concentration and temperature, *J. Food Eng.* 101 (3) (2010) 236–243.
  - [27] A. Zameni, M. Kashaninejad, M. Aalami, F. Salehi, Effect of thermal and freezing treatments on rheological, textural and color properties of basil seed gum, *J. Food Sci. Technol.* 52 (9) (2015) 5914–5921.
  - [28] S. Naji-Tabasi, S.M.A. Razavi, New studies on basil (*ocimum basilicum* L.) seed gum: part III-steady and dynamic shear rheology, *Food Hydrocolloids* 67 (2017) 243–250.
  - [29] H. Gamal, S. Elkhatatny, S. Basfar, A. Al-Majed, Effect of pH on rheological and filtration properties of water-based drilling fluid based on bentonite, *Sustain. Times* 11 (23) (2019) 1–13.
  - [30] A. Garcia-Hernandez, C. Lobato-Calleros, E.J. Vernon-Carter, E. Sosa-Hernandez, J. Alvarez-Ramirez, Effects of clay concentration on the morphology and rheological properties of xanthan gum-based hydrogels reinforced with montmorillonite particles, *J. Appl. Polym. Sci.* 134 (8) (2017) 1–10.
  - [31] J.P. Plank, J.V. Hamberger, Field Experience with a Novel Calcium-Tolerant Fluid-Loss Additive for Drilling Muds, SPE-18372-MS, European Petroleum Conference, London, 1988, pp. 16–19 October.
  - [32] S. Shah, S.A. Heinle, J.E. Glass, Water-soluble polymer adsorption from saline solutions, SPE-13561-MS, in: SPE Oilfield and Geothermal Chemistry Symposium, Arizona, 1985, 9–11 March.
  - [33] H.M. Ahmad, M.S. Kamal, M.A. Al-Harhi, Rheological and filtration properties of clay-polymer systems: impact of polymer structure, *Appl. Clay Sci.* 160 (2018) 226–237.
  - [34] R. Farahmandfar, S. Naji-Tabasi, Influence of different salts on rheological and functional properties of basil (*Ocimum basilicum* L.) seed gum, *Int. J. Biol. Macromol.* 149 (2020) 101–107.
  - [35] A. Audibert, L. Rousseau, J. Kieffer, Novel high-pressure/high temperature fluid loss reducer for water-based formulation, SPE-50724-MS, in: SPE International Symposium on Oilfield Chemistry, Texas, 1999, 16–19 February.
  - [36] J. Elward-Berry, J.B. Darby, Rheologically stable, nontoxic, high-temperature water-base drilling fluid, *SPE Drill. Completion* 12 (3) (1997) 158–162.
  - [37] A. Rafe, M.A. Razavi, R. Farhoosh, Rheology and microstructure of basil seed gum and  $\beta$ -lactoglobulin mixed gels, *Food Hydrocolloids* 30 (1) (2013) 134–142.
  - [38] M.R.P. Rao, M. Khambete, H.N. Lunavat, Study of rheological properties of psyllium polysaccharide and its evaluation as suspending agent, *Int. J. PharmTech Res.* 3 (2) (2011) 1191–1197.
  - [39] S. Naji-Tabasi, S.M.A. Razavi, H. Mehditabar, Fabrication of basil seed gum nanoparticles as a novel oral delivery system of glutathione, *Carbohydr. Polym.* 157 (2017) 1703–1713.
  - [40] T. Yalçın, A. Alemdar, Ö.I. Ece, N. Güngör, The viscosity and zeta potential of bentonite suspensions in presence of anionic surfactants, *Mater. Lett.* 57 (2) (2002) 420–424.
  - [41] R.N. Yong, D. Mourato, Influence of polysaccharides on kaolinite structure and properties in a kaolinite-water system, *Can. Geotech. J.* 27 (6) (1990) 774–788.
  - [42] O. Duman, S. Tun, Electrokinetic and rheological properties of Na-bentonite in some electrolyte solutions, *Microporous Mesoporous Mater.* 117 (1–2) (2009) 331–338.
  - [43] J. Labille, F. Thomas, M. Milas, Flocculation of colloidal clay by bacterial polysaccharides: effect of macromolecule charge and structure, *J. Colloid Interf.* 284 (1) (2005) 149–156.
  - [44] J.P. Plank, F.A. Gossen, Visualization of fluid-loss polymers in drilling-mud filter cakes, SPE-19534-PA, *SPE Drill. Eng.* 6 (3) (1991) 203–208.
  - [45] H.M. Ahmad, M.S. Kamal, M.A. Al-Harhi, Rheological and filtration properties of clay-polymer systems: impact of polymer structure, *Appl. Clay Sci.* 160 (2018) 226–237.
  - [46] O.H. Houwen, Chemical characterization of CMC and its relationship to drilling-mud rheology and fluid loss, SPE-20000-PA, *SPE Drill. Completion* 8 (3) (1993) 157–164.
  - [47] R.C. Navarrete, R.E. Himes, J.M. Seheult, Applications of Xanthan gum in fluid-loss control and related formation damage, SPE 59535, in: SPE Permian Basin Oil and Gas Recovery Conference, Texas, 12–23 March, 2000.
  - [48] Q. Zhou, G. Meng, N. Wu, N. Zhou, B. Chen, F. Li, Q. Huang, Dipping into a drink: basil-seed supported silver nanoparticles as surface-enhanced Raman scattering substrates for toxic molecule detection, *Sensor. Actuator. B Chem.* 223 (2016) 447–452.
  - [49] K.M. Dontsova, J.M. Bigham, Anionic polysaccharide sorption by clay minerals, *Soil Sci. Soc. Am. J.* 69 (2005) 1026–1035.
  - [50] S.A. Heinle, S. Shah, J.E. Glass, Influence of Water-Soluble Polymers on the Filtration Control of Bentonite Muds, *Water-Soluble Polymers*, 1986, pp. 183–196 (Chapter 11).